ACS Medicinal Chemistry Letters

Letter

pubs.acs.org/acsmedchemlett

Potent Small Agonists of Protease Activated Receptor 2

Mei-Kwan Yau,[†] Jacky Y. Suen,[†] Weijun Xu,[†] Junxian Lim,[†] Ligong Liu,[†] Mark N. Adams,[‡] Yaowu He,[‡] John D. Hooper,[‡] Robert C. Reid,[†] and David P. Fairlie*[,†]

[†]Institute for Molecular Bioscience, The University of Queensland, Brisbane, Qld 4072, Australia

[‡]Translational Research Institute, Mater Research Institute, The University of Queensland, Woolloongabba, Qld 4102, Australia

Supporting Information

ABSTRACT: Many proteases cut the PAR2 N-terminus resulting in conformational changes that activate cells. Synthetic peptides corresponding to newly exposed N-terminal sequences of PAR2 also activate the receptor at micromolar concentrations. PAR2-selective small molecules reported here induce PAR2-mediated intracellular calcium signaling at nanomolar concentrations (EC_{50} = 15−100 nM, iCa^{2+}, CHO-hPAR2 cells). These are the most potent and efficient small molecule ligands to activate PAR2-mediated calcium release and chemotaxis, including for human breast and prostate cancer cells.

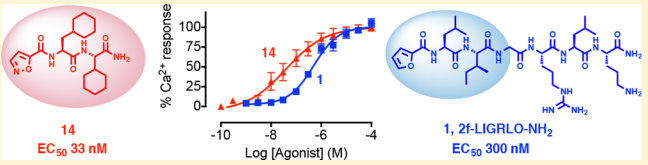

KEYWORDS: *Protease activated receptor 2, agonist, cyclohexylglycine, structure−activity relationships*

Protease-activated receptors (PARs) are class A GPCRs, self-activated by their newly exposed N-terminus following cleavage by proteases. Protease-activated receptor 2 (PAR2) is one of four PAR subtypes and its N-terminus is cleaved by enzymes (e.g., trypsin, tryptase, factor Xa/VIIa, granzyme A) at the R^{36}-S^{37} cleavage site to reveal an activating sequence S^{37}LIGKV (human) or S^{37}LIGRL (rodent).[1−3] Some proteases cleave elsewhere, with the cysteine protease cathepsin S cleaving at G^{40}-K^{41} and E^{56}-T^{57}.[4,5] PAR2 has been implicated in disease models of, for example, arthritis,[6,7] inflammatory bowel disease,[8,9] asthma,[10,11] cardiovascular diseases,[12,13] cancers,[14,15] and metabolic dysfunction.[16,17] However, roles for PAR2 in human diseases remain uncertain, with both pro- and anti-inflammatory properties as well as protective and disease-promoting roles reported.[1,18,19]

Synthetic agonists and antagonists are therefore valuable tools for investigating PAR2 functions *in vivo*. Most ligands used to date to evaluate PAR2 biology have been peptides, which tend to be metabolically unstable.[20,21] Synthetic hexapeptide SLIGRL-NH_2, which is more potent than the native sequence SLIGKV-NH_2 in activating human PAR2 on cells, has been the most widely used peptide agonist, but it is only active at micromolar concentrations.[20] Extensive structure−activity relationships, performed on this peptide by replacing each amino acid with other natural/unnatural amino acids, have generated more potent peptides. For example, the N-terminal serine has been replaced by a heterocycle, such as 2-furoyl (2f);[22] 4-(2-methyloxazolyl), 5-isoxazolyl (Isox), 2-pyrazolyl, 2-pyridolyl, 3-pyridolyl, 2-benzofuranoyl, 2-naphthoyl, 2-benzothienyl,[23] and 2-aminothiazol-4-yl (2-at).[24] Heptapeptides like 2f-LIGRLO-NH_2 (**1**, Figure 1) and X-LIGRLI-NH_2 (**2**, with different heterocycles) were reported to be selective agonists for PAR2 with EC_{50} between 0.1−0.8 μM measured by intracellular calcium (iCa^{2+}) release in various cell lines (e.g., HCT-15, HT29, 16HBE14o-).[22−24] Linking a hexadecyl lipid via three polyethylene glycol (PEG) spacer units to the ornithine amine side chain (**3**) or at the C-terminal of 2f-LIGRL also evidently increases agonist potency to nanomolar concentrations in an iCa^{2+} assay on 16HBE14o- cells.[25] A few nonpeptidic PAR2 agonists (**4**, AC-55541 and AC-264613) were also reported with potency similar to **1** (EC_{50} 100−300 nM, iCa^{2+}).[26−28] Our goal here was to minimize size, reduce polar atoms and polar surface area, and reduce rotatable bonds yet still produce a potent, rule-of-five

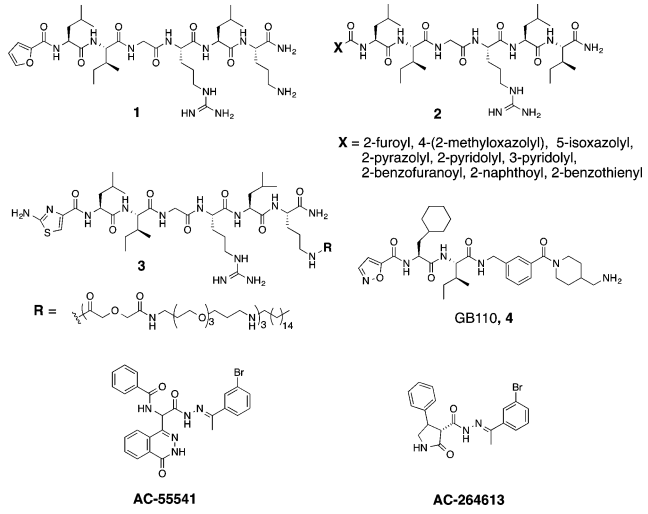

Figure 1. Known synthetic PAR2 agonists.[22,23,25−28]

Received: November 8, 2015
Accepted: November 30, 2015
Published: November 30, 2015

DOI: 10.1021/acsmedchemlett.5b00429
ACS Med. Chem. Lett. 2016, 7, 105−110

compliant compound with higher potency and ligand efficiency than **1**−**4** and greater stability in biological media.

The PAR2 peptide agonist **1** was sequentially truncated to reduce the size of the peptide, and the first three residues were replaced with Isox-Cha-Ile, a component of **4**. Agonist activities for its derivatives (Table 1) were evaluated, using Chinese hamster ovary cells stably expressing human PAR2 (CHO-hPAR2), for intracellular Ca^{2+} release since this signaling via PAR2 has been implicated in multiple diseases.[7,9,18] In these cells, synthetic peptide SLIGKV-NH_2 was 10-fold or more less potent (EC_{50} 3 μM) than **1** and **4**. Peptide **7** was less potent than **8**, suggesting that the extra C-terminal leucine was unnecessary. Truncating **8** to **9** did not affect agonist activity, but truncation to **10** reduced the potency to that of **1** and **4**.

Table 1. PAR2 Agonist Activity in Inducing Ca^{2+} Release in CHO-hPAR2 Cells

#	compd	pEC_{50} ± SEM	EC_{50} (nM)
1	2f-LIGRLO-NH_2	6.5 ± 0.1	300
4	GB110	6.7 ± 0.2	200
5	trypsin	8.9 ± 0.3	1
6	SLIGKV-NH_2	5.5 ± 0.1	3000
7	Isox-Cha-Ile-GRL-NH_2	6.7 ± 0.1	200
8	Isox-Cha-Ile-GR-NH_2	7.1 ± 0.2	80
9	Isox-Cha-Ile-G-NH_2	7.0 ± 0.2	95
10	Isox-Cha-Ile-NH_2	6.4 ± 0.2	400
11	Isox-Cha-Chg-GRL-NH_2	7.1 ± 0.1	80
12	Isox-Cha-Chg-GR-NH_2	7.2 ± 0.3	62
13	Isox-Cha-Chg-G-NH_2	7.7 ± 0.2	18
14	Isox-Cha-Chg-NH_2	7.5 ± 0.3	33
15	H_2N-Cha-Chg-GR-NH_2	<4.0	>100000
16	H_2N-Chg-GR- NH_2	<4.0	>100000

Docking of **10** into a PAR2 homology model (Supporting Information, SI), generated by sequence alignment of PAR2 with the crystal structure of nociceptin/orphanin FQ receptor (pdb code 4EA3), suggested that the binding pocket surrounding the Ile-binding site is large and can accommodate a bulkier substituent. Cyclohexylglycine (Chg) replaced Ile in compounds **7**−**10** to produce **11**−**14**. Compounds **13** and **14**, with the fewest residues, were more potent agonists in inducing Ca^{2+} release than **11** and **12** (Table 1). This was despite the presence in **11** and **12** of an arginine, which often forms strong hydrogen bonds or electrostatic interactions within proteins.

Removing Isox and Cha (**15** and **16**) almost abolished activity, suggesting that these groups were more important than arginine for interactions in the ligand binding site. The minimal pharmacophore involved three residues, Isox-Cha-Ile-NH_2 (**10**) and Isox-Cha-Chg-NH_2 (**14**, AY77), the latter being ∼10-fold more potent for inducing intracellular Ca^{2+} release.

Agonist **14** was next docked into the PAR2 homology model and the best fitting docked pose of the ligand was selected for further analysis. We were interested in learning what interactions between **14** and PAR2 were responsible for activating the PAR2-Ca^{2+} pathway. From the ligand docking experiments, the nitrogen of isoxazole was predicted to form a hydrogen bond with Y82, while the terminal amide may also interacted with residues D228 and Y156 through hydrogen bonding. In addition, one of the amide carbonyl groups of **14** was predicted to interact with Y156 (Figure 2a). The surface view of the PAR2 homology model suggested that the isoxazole, Cha, and Chg bound into three distinct pockets (Figure 2b). Compound **14** was also docked into a PAR2 homology model derived from the PAR1 crystal structure (results not shown); however, the docked pose did not agree with the PAR2 mutagenesis results unlike this model (Figures 2b−d).

To validate the binding site and pose of **14**, the agonist activity of this compound was investigated in CHO cells transfected with mutant PAR2 (Y82A, Y156A, D228A, L307A, Y326A) (Figure 2c). Mutations of Y82, Y326, D228, or Y156 to alanine resulted in loss of H-bond interactions of these residues with **14**, its agonist activity in inducing iCa^{2+} being significantly reduced by nearly 100-fold. Additionally, a L307A mutation suggested a larger binding cavity for **14** so that Chg could not fit as snugly into the pocket, resulting in loss of activity. Residues Y82, D228, and Y156 were in close proximity (within 2.0−3.0 Å, Figure 2d) to the ligand, consistent with H-bonding, but Y326 was located further away from the proposed binding site of **14** and may not form a direct H-bond with ligand. However, **14** may interact with Y326 through water-mediated H-bonding, consistent with reduced agonist activity in the Y326A mutant cells. To our knowledge, no binding site for a PAR2 ligand has ever been clearly elucidated before. To further support the binding mode of **14**, its amide NH_2 was methylated to give Isox-Cha-Chg-NMe_2, which was less active than **14** (data not shown) suggesting that the C-terminal NH_2 may be involved in H-bonding. Compound **14** is the first small molecule agonist (MW < 500) reported to activate PAR2 at low nanomolar concentrations. In terms of ligand efficiency (PEI, Table 2), **14** is superior to other PAR2 agonists. Agonist **14** was also more stable in rat plasma than peptides **1** and **6** (Figure 3a), making it potentially more valuable for physiologically relevant studies.

Table 2. Percentage Efficiency Index (PEI)

compd	MW (Da)	PEI[a]
1	778	0.51
3	2003	0.35
4	609	0.82
13	461	1.52
14	404	1.73

[a]PEI calculated as fraction of Ca^{2+} (i.e., 50% = 0.5) induced by 100 nM agonist divided by MW (kDa).[29]

The selectivity of agonist **14** was evaluated in CHO-hPAR2 cells compared to CHO cells without PAR2 transfection. In CHO-hPAR2 cells, agonist **14** was 10-fold more potent (EC_{50} 33 nM) than peptide agonist **1** (EC_{50} 300 nM) and neither of these agonists induced any iCa^{2+} release at 100 μM concentrations in $PAR2^{-/-}$-CHO cells, revealing that they both activate Ca^{2+} release selectively via PAR2 (Figure 3b).

Some synthetic peptides have been shown to cross-react with PAR1 and PAR2 receptors.[20] Therefore, **14** was assessed for receptor subtype selectivity in a desensitization assay using human prostate cancer cells (PC3) that expressed both PAR1 and PAR2 (SI, Figure S1).

In this desensitization experiment, cells were first exposed to **1** (a selective PAR2 agonist) at 25 μM and induced Ca^{2+} release, whereas there was no response to a second treatment with this same agonist (SI, Figure S1a). This indicated that the PAR2 on the cell membrane had been desensitized by the first agonist treatment and thus did not respond to the second treatment. By contrast, a PAR1 agonist (TFLLR-NH_2) was able

DOI: 10.1021/acsmedchemlett.5b00429
ACS Med. Chem. Lett. 2016, 7, 105−110

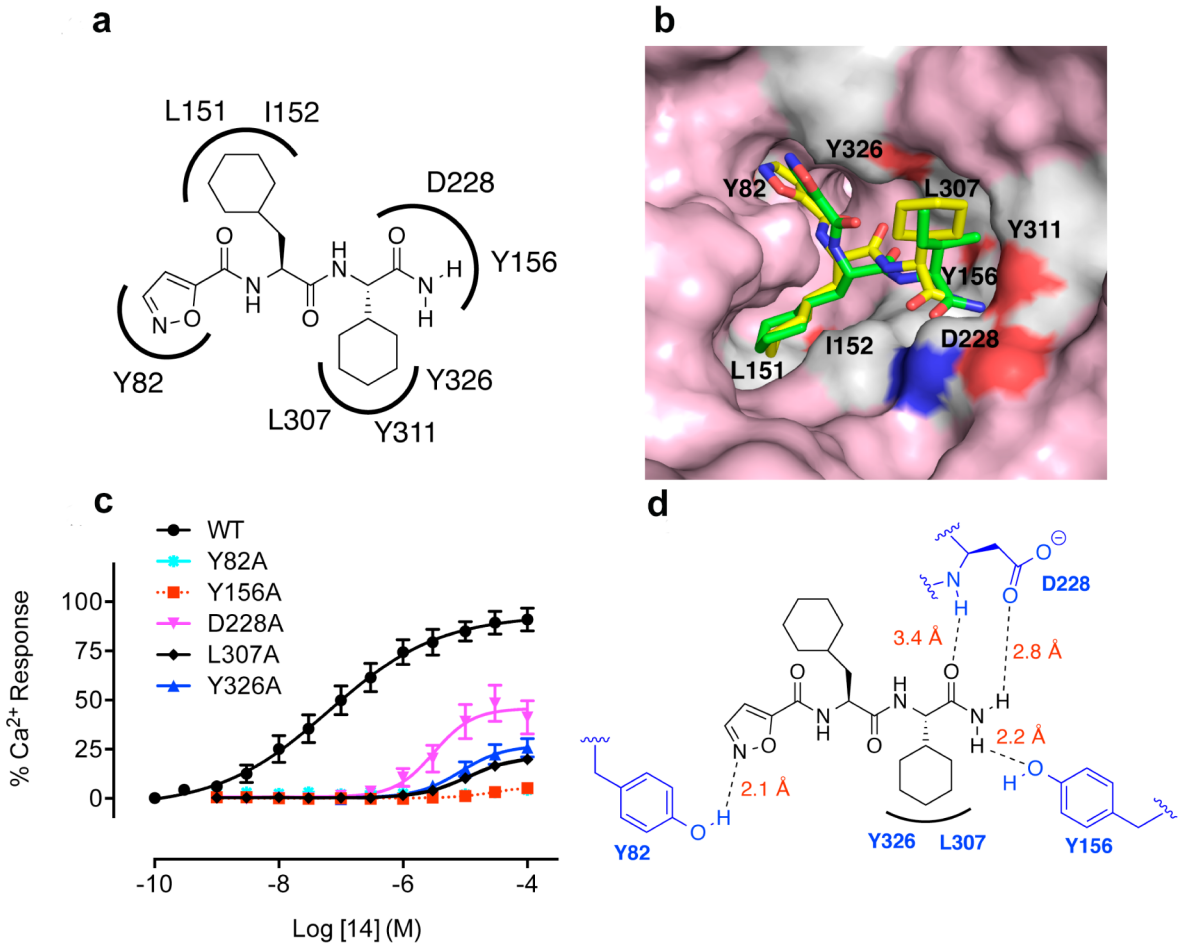

Figure 2. Predicted binding mode for agonist **14** in a PAR2 homology model derived from nociceptin/orphanin FQ receptor (pdb code 4EA3). (A) Agonist AY77 (**14**) is predicted to form multiple hydrogen bonds and hydrophobic interactions with PAR2. (B) Surface view of PAR2 model showing Isox, Cha, and Chg components occupying three distinct binding pockets. (C) iCa^{2+} responses induced by agonist **14** were significantly reduced in PAR2 mutants Y156A, Y326A, D228A, L307A, and Y82A compared to wild-type (WT), suggesting that these residues interact with **14**. Each data point is mean ± SEM of 3−5 independent experiments. (D) The C-terminal amide NH_2 of **14** forms hydrogen bonds with Y156 and D228. The cyclohexylglycine may make a hydrophobic interaction with L307 and the amide carbonyl of Cha may form a water mediated H-bond with Y326. Isoxazole may form a H-bond with Y82.

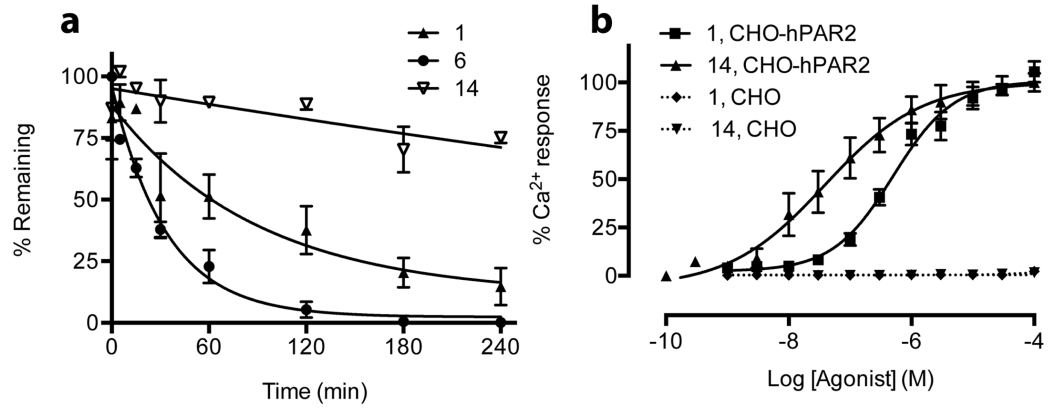

Figure 3. (a) Agonist **14** was stable in rat plasma after 4 h (pH 7.4, 37 °C, initial concentration 1 μM) compared to peptides **1** and **6**. The plasma samples were analyzed by LCMS (n = 3). (b) Agonists **1** and **14** (AY77) activate Ca^{2+} release via PAR2. Experiments were performed in CHO-hPAR2 cells (solid lines) versus CHO cells ($PAR2^{-/-}$, dotted lines), $n \geq 3$. Each data point represents mean ± SEM.

to activate the PAR2-desensitized cells causing a second calcium signal following initial treatment with **1** (SI, Figure S1b). Compound **14**, at up to 10 μM, did not trigger this second calcium signal after initial PAR2 desensitization with **1** (SI, Figure S1c), consistent with **14** being selective for PAR2 over PAR1.

The functions of PAR2 agonists were further evaluated in human breast cancer cells (MDA-MB-231), known to express

DOI: 10.1021/acsmedchemlett.5b00429
ACS Med. Chem. Lett. 2016, 7, 105−110

PAR2.[30] Activation of PAR2 induced by agonists **1** or **14** at 100 nM caused chemotactic migration that was attenuated by treating with an anti-PAR2 antibody (SAM11). This is consistent with the observed cell migration being PAR2-specific, the small agonist **14** being as effective and as potent as the larger peptide agonist **1** in activating PAR2 in this assay (Figure 4).

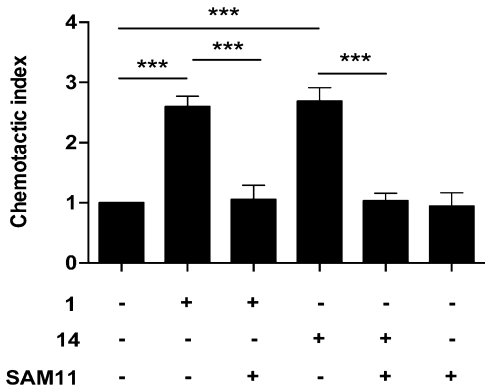

Figure 4. PAR2-activated chemotaxis in MDA-MB-231 breast cancer cells. Compounds **1** and **14** (100 nM) induced chemotaxis in a transwell migration assay. Preincubating cells with PAR2 antibody SAM11 (1 μg/mL) 30 min prior to agonist addition resulted in inhibition of chemotaxis. The chemotactic index is the ratio of agonist to random migration (24 h) through a 5 μm membrane, mean ± SEM, ***$p < 0.001$.

Small molecules described here (e.g., **13**, **14**) are the most potent PAR2 agonists reported to induce Ca^{2+} release. Receptor modeling in combination with human PAR2 mutants transfected into CHO cells were used to probe the mechanism of Ca^{2+} release induced by **14**. Putative interactions, predicted from modeling studies, between **14** and PAR2 residues Y82, Y156, D228, L307, and Y326 were experimentally supported by PAR2 mutagenesis data. Effects of **14** were also measured on cancer cells, including chemotaxis of breast cancer cells and Ca^{2+} desensitization of prostate cancer cells. Compound **14** is a potent, effective, and selective small molecule (MW 404) agonist for PAR2 with the highest ligand efficiency yet known. It is more stable than peptides in rat plasma, activates PAR2-mediated Ca^{2+} signaling with high potency (EC_{50} 33 nM, CHO-hPAR2), and has agonist activity on two human cancer cell lines. Compound **14** is a valuable new tool for interrogating PAR2 physiology[3] and a new pharmacophore to exploit for creating potent agonists and antagonists as prospective drug candidates that selectively modulate PAR2.

EXPERIMENTAL PROCEDURES

General Methods. Reagents were purchased from Sigma-Aldrich or Chem-Impex Int., Inc. Compound purity was assessed by NMR spectroscopy, rpHPLC, and high-resolution mass spectra (HRMS). All assayed compounds were ≥95% pure, as determined by rpHPLC (UV detection at 214, 230, and 254 nm). Other experimental methods and characterization data of all compounds, except **13** and **14**, are reported in Supporting Information. Synthetic compounds **13** and **14** are characterized below.

Solid-Phase Synthesis. All compounds were synthesized on solid phase by standard Fmoc SPPS procedures using Rink amide resin (100–300 mg, 0.70 mmol/g), purified by reversed phase HPLC to >95% purity, and characterized by high resolution MS and NMR spectroscopy.

Isox-Cha-Chg-G-NH$_2$ ***(13)***. t_R = 9.1 min. HRMS: $[MNa]^+$ 484.2530 (calc. for $C_{23}H_{36}N_5O_5^+$) 484.2533 (found). ^{1}H NMR (600 MHz, DMSO-d_6), δ 0.83–1.22 (m, 10H), 1.31 (m, 1H), 1.51–1.75 (m, 13H), 3.54–3.70 (2 sets of dd, J = 5.7 Hz, 2H), 4.11 (t, J = 7.9 Hz, 1H), 4.57 (m, 1H), 7.05 (br s, 1H), 7.17 (d, J = 1.9 Hz, 1H), 7.19 (br s, 1H), 8.00 (d, J = 8.2 Hz, 1H), 8.14 (t, J = 5.7 Hz, 1H), 8.75 (d, J = 1.9 Hz, 1H), 8.99 (d, J = 8.2 Hz, 1H). ^{13}C NMR (150 MHz, DMSO-d_6), δ 25.5, 25.6, 25.7, 25.8, 26.0, 28.2, 29.0, 31.7, 33.2, 33.6, 38.5, 41.7, 50.2, 57.6, 106.1, 151.7, 155.4, 162.3, 170.6, 170.8, 171.5.

Isox-Cha-Chg-NH$_2$ ***(14)***. t_R = 9.4 min. HRMS: $[MH]^+$ 405.2496 (calc. for $C_{21}H_{33}N_4O_4^+$) 405.2498 (found). ^{1}H NMR (600 MHz, DMSO-d_6), δ 0.82–1.20 (m, 9H), 1.29 (m, 1H), 1.50–1.59 (m, 5H), 1.59–1.71 (m, 9H), 4.08 (t, J = 7.7 Hz, 1H), 4.53 (m, 1H), 7.00 (br s, 1H), 7.14 (d, J = 1.9 Hz, 1H), 7.36 (br s, 1H), 7.77 (d, J = 9.4 Hz, 1H), 8.73 (d, J = 1.7 Hz, 1H), 8.97 (d, J = 8.5 Hz, 1H). ^{13}C NMR (150 MHz, DMSO-d_6), δ 25.9, 26.0, 26.1, 26.2, 26.4, 28.4, 29.6, 32.1, 33.6, 34.1, 39.1, 51.4, 57.3, 106.6, 152.2, 155.8, 162.8, 171.5, 173.0.

Cell Culture, Expression Constructs, and Transfections. Methods for preparation of Chinese hamster ovary (CHO), PC3, and MDA-MB-231 cancer cells are described in the Supporting Information.

Intracellular Calcium Release Assay. Cells were plated at ~5 × 10^4 cells/well in a 96-well clear-bottom black-wall assay plate (Corning) and incubated overnight at 37 °C. Before assay, the medium was removed, and cells were incubated with dye-loading buffer (12 mL HBSS buffer, 4 μM Fluo-3 AM, 25 μL of Pluronic acid F-127, 1% FBS) for 1 h at 37 °C. Cells were washed once (HBSS buffer containing 2.5 mM probenecid and 20 mM HEPES, pH 7.4). Stock solutions of compounds in DMSO were diluted with HBSS buffer to give assay concentrations. Agonist activity was measured at a range of concentrations of test compound (50 μL) added to cells in 50 μL of HBSS buffer. Intracellular Ca^{2+} was monitored for 300 s (excitation 495 nm, emission 520 nm) after injecting compound. Duplicate measurements for each data point were reported as means ± SEM from multiple experiments. Changes in fluorescence (% response) were plotted against log[compound]. Half maximal effective concentrations (EC_{50}) were derived from concentration–response curves using a nonlinear regression curve fitting (Graphpad Prism v6). Calcimycin (A23187, Invitrogen) was used to measure maximum fluorescence; individual results were normalized.

Rat Plasma Stability Assay. Compounds in DMSO (5 μL, 100 μM) were added to a 1:1 mixture of PBS and rat plasma (495 μL) at 37 °C. At intervals of 0, 5, 15, 30, 60, 120, 180, and 240 min, 50 μL was removed and added to 150 μL of MeCN. Samples were centrifuged (2500 rpm, 5 min) and supernatant (50 μL) analyzed by UPLC-MS. Data were plotted as % peak area of samples at t = 0 min.

Transwell Cell Migration. A transwell polycarbonate filter insert with 5 μm membrane was used to determine cell migration. Both sides of the membrane were coated with collagen (1 mg/mL, 50 μL) for 2 min before air-drying. Cells were lifted with nonenzymatic cell dissociation solution and resuspended in 0.1% BSA serum-free L-15. Cells were seeded at 2.5 × 10^5 cells/insert and allowed to incubate (3 h, 37 °C). Then, 700 μL of 0.1% BSA serum-free L-15 with 100 nM of PAR2 agonist was added to the bottom chamber and incubated for 24 h. For inhibition of chemotaxis, SAM11 (1 μg/mL) was preincubated for 30 min prior to adding agonist. Cells on top of the membrane were removed with a cotton swab and fixed in 4% PFA. The insert was washed 2× in PBS and stained with 1% crystal violet. Migrated cells on the underside of the membrane were counted using a Nikon Ti–U inverted brightfield microscope.

Molecular Modeling. A homology model of human PAR2 was generated by alignment with Nociceptin/orphanin FQ receptor structure (pdb code 4EA3). Methods used for generating the PAR2 homology model and docking ligands are in Supporting Information.

DOI: 10.1021/acsmedchemlett.5b00429
ACS Med. Chem. Lett. 2016, 7, 105–110

■ ASSOCIATED CONTENT

Supporting Information

The Supporting Information is available free of charge on the ACS Publications website at DOI: 10.1021/acsmedchemlett.5b00429.

Desensitization experimental results, general experimental methods, compound characterization data (NMR, HPLC, HRMS), and methods used for generating PAR2 homology model (PDF)

■ AUTHOR INFORMATION

Corresponding Author

*Tel: +61733462989. Fax: +61733462990. E-mail: d.fairlie@uq.edu.au.

Author Contributions

M.K.Y. and D.P.F. conceived experiments, analyzed results, and wrote the paper. M.N.A., Y.H., and J.D.H. transfected CHO cells with PAR2 mutants. M.K.Y., J.Y.S., W.X., J.L., L.L., and R.R. performed all experiments.

Funding

D.P.F. acknowledges NHMRC for grants 1047759, 1000745, 569595 and an SPRF fellowship (1027369); the Queensland Government for a CIF grant; and ARC for DP130100629 and CE140100011 grants and the ARC Centre of Excellence in Advanced Molecular Imaging. M.A. received an Australian Post-Graduate Award. J.D.H. holds ARC Future Fellowship FT120100917.

Notes

The authors declare the following competing financial interest(s): D.P.F., L.L., M.K.Y., J.Y.S., and R.R. are named inventors on US Patent 8,927,503 and are co-authors on this manuscript. The patent is owned by the University of Queensland and concerns agonists and antagonists of PAR2.

■ ACKNOWLEDGMENTS

We thank the ACRF Imaging Facility (Brisbane) for use of microscopes and Prof. K. K. Khanna (QIMR-Berghofer Institute, Brisbane) for MDA-MB-231 cells.

■ ABBREVIATIONS

2f, 2-furoyl; Cha, cyclohexylalanine; Chg, cyclohexylglycine; CHO, Chinese hamster ovary cells; 16HBE14o-, SV40-transformed human bronchial epithelial cells; H-bond, hydrogen bond; HBSS, Hank's balanced salt solution; HCT-15, human colon carcinoma cells; HEPES, (4-(2-hydroxyethyl)-1-piperazineethanesulfonic acid; HT29, human colonic adenocarcinoma cells; iCa^{2+}, intracellular calcium; Isox, 5-isoxazole; MDA-MB-231, human breast adenocarcinoma cells; MW, molecular weight; PAR2, protease activated receptor 2; PC3, human prostate cancer cells; PEG, polyethylene glycol; PEI, percent efficiency index; TM, transmembrane; WT, wild-type

■ REFERENCES

(1) Adams, M. N.; Ramachandran, R.; Yau, M. K.; Suen, J. Y.; Fairlie, D. P.; Hollenberg, M. D.; Hooper, J. D. Structure, function and pathophysiology of protease activated receptors. *Pharmacol. Ther.* **2011**, *130*, 248−282.

(2) Rothmeier, A. S.; Ruf, W. Protease-activated receptor 2 signaling in inflammation. *Semin. Immunopathol.* **2012**, *34*, 133−149.

(3) Yau, M. K.; Liu, L.; Fairlie, D. P. Toward drugs for protease-activated receptor 2 (PAR2). *J. Med. Chem.* **2013**, *56*, 7477−7497.

(4) Elmariah, S. B.; Reddy, V. B.; Lerner, E. A.; Cathepsin, S. Signals via PAR2 and Generates a Novel Tethered Ligand Receptor Agonist. *PLoS One* **2014**, *9*, e99702.

(5) Zhao, P.; Lieu, T.; Barlow, N.; Metcalf, M.; Veldhuis, N. A.; Jensen, D. D.; Kocan, M.; Sostegni, S.; Haerteis, S.; Baraznenok, V.; Henderson, I.; Lindstrom, E.; Guerrero-Alba, R.; Valdez-Morales, E. E.; Liedtke, W.; McIntyre, P.; Vanner, S. J.; Korbmacher, C.; Bunnett, N. W. Cathepsin S causes inflammatory pain via biased agonism of PAR2 and TRPV4. *J. Biol. Chem.* **2014**, *289*, 27215−27234.

(6) Ferrell, W. R.; Lockhart, J. C.; Kelso, E. B.; Dunning, L.; Plevin, R.; Meek, S. E.; Smith, A. J.; Hunter, G. D.; McLean, J. S.; McGarry, F.; Ramage, R.; Jiang, L.; Kanke, T.; Kawagoe, J. Essential role for proteinase-activated receptor-2 in arthritis. *J. Clin. Invest.* **2003**, *111*, 35−41.

(7) Lohman, R. J.; Cotterell, A. J.; Barry, G. D.; Liu, L.; Suen, J. Y.; Vesey, D. A.; Fairlie, D. P. An antagonist of human protease activated receptor-2 attenuates PAR2 signaling, macrophage activation, mast cell degranulation, and collagen-induced arthritis in rats. *FASEB J.* **2012**, *26*, 2877−2887.

(8) Hansen, K. K.; Sherman, P. M.; Cellars, L.; Andrade-Gordon, P.; Pan, Z.; Baruch, A.; Wallace, J. L.; Hollenberg, M. D.; Vergnolle, N. A major role for proteolytic activity and proteinase-activated receptor-2 in the pathogenesis of infectious colitis. *Proc. Natl. Acad. Sci. U. S. A.* **2005**, *102*, 8363−8368.

(9) Lohman, R. J.; Cotterell, A. J.; Suen, J.; Liu, L.; Do, A. T.; Vesey, D. A.; Fairlie, D. P. Antagonism of protease-activated receptor 2 protects against experimental colitis. *J. Pharmacol. Exp. Ther.* **2012**, *340*, 256−265.

(10) Cocks, T. M.; Fong, B.; Chow, J. M.; Anderson, G. P.; Frauman, A. G.; Goldie, R. G.; Henry, P. J.; Carr, M. J.; Hamilton, J. R.; Moffatt, J. D. A protective role for protease-activated receptors in the airways. *Nature* **1999**, *398*, 156−160.

(11) Cocks, T. M.; Moffatt, J. D. Protease-activated receptor-2 (PAR2) in the airways. *Pulm. Pharmacol. Ther.* **2001**, *14*, 183−191.

(12) Damiano, B. P.; Cheung, W. M.; Santulli, R. J.; Fung-Leung, W. P.; Ngo, K.; Ye, R. D.; Darrow, A. L.; Derian, C. K.; de Garavilla, L.; Andrade-Gordon, P. Cardiovascular responses mediated by protease-activated receptor-2 (PAR-2) and thrombin receptor (PAR-1) are distinguished in mice deficient in PAR-2 or PAR-1. *J. Pharmacol. Exp. Ther.* **1999**, *288*, 671−678.

(13) Antoniak, S.; Rojas, M.; Spring, D.; Bullard, T. A.; Verrier, E. D.; Blaxall, B. C.; Mackman, N.; Pawlinski, R. Protease-activated receptor 2 deficiency reduces cardiac ischemia/reperfusion injury. *Arterioscler., Thromb., Vasc. Biol.* **2010**, *30*, 2136−2142.

(14) Ryden, L.; Grabau, D.; Schaffner, F.; Jonsson, P. E.; Ruf, W.; Belting, M. Evidence for tissue factor phosphorylation and its correlation with protease-activated receptor expression and the prognosis of primary breast cancer. *Int. J. Cancer* **2010**, *126*, 2330−2340.

(15) Lam, D. K.; Dang, D.; Zhang, J.; Dolan, J. C.; Schmidt, B. L. Novel animal models of acute and chronic cancer pain: a pivotal role for PAR2. *J. Neurosci.* **2012**, *32*, 14178−14183.

(16) Badeanlou, L.; Furlan-Freguia, C.; Yang, G.; Ruf, W.; Samad, F. Tissue factor-protease-activated receptor 2 signaling promotes diet-induced obesity and adipose inflammation. *Nat. Med.* **2011**, *17*, 1490−1497.

(17) Lim, J.; Iyer, A.; Liu, L.; Suen, J. Y.; Lohman, R. J.; Seow, V.; Yau, M. K.; Brown, L.; Fairlie, D. P. Diet-induced obesity, adipose inflammation, and metabolic dysfunction correlating with PAR2 expression are attenuated by PAR2 antagonism. *FASEB J.* **2013**, *27*, 4757−4767.

(18) Suen, J. Y.; Cotterell, A.; Lohman, R. J.; Lim, J.; Han, A.; Yau, M. K.; Liu, L.; Cooper, M. A.; Vesey, D. A.; Fairlie, D. P. Pathway Selective Antagonism Of Proteinase Activated Receptor 2. *Br. J. Pharmacol.* **2014**, *171*, 4112−4124.

(19) Hollenberg, M. D.; Mihara, K.; Polley, D.; Suen, J. Y.; Han, A.; Fairlie, D. P.; Ramachandran, R. Biased signalling and proteinase-activated receptors (PARs): targeting inflammatory disease. *Br. J. Pharmacol.* **2014**, *171*, 1180−1194.

DOI: 10.1021/acsmedchemlett.5b00429
ACS Med. Chem. Lett. 2016, 7, 105−110

(20) Maryanoff, B. E.; Santulli, R. J.; McComsey, D. F.; Hoekstra, W. J.; Hoey, K.; Smith, C. E.; Addo, M.; Darrow, A. L.; Andrade-Gordon, P. Protease-activated receptor-2 (PAR-2): structure-function study of receptor activation by diverse peptides related to tethered-ligand epitopes. *Arch. Biochem. Biophys.* **2001**, *386*, 195−204.
(21) Devlin, M. G.; Pfeiffer, B.; Flanagan, B.; Beyer, R. L.; Cocks, T. M.; Fairlie, D. P. Hepta and octapeptide agonists of protease-activated receptor 2. *J. Pept. Sci.* **2007**, *13*, 856−861.
(22) McGuire, J. J.; Saifeddine, M.; Triggle, C. R.; Sun, K.; Hollenberg, M. D. 2-furoyl-LIGRLO-amide: a potent and selective proteinase-activated receptor 2 agonist. *J. Pharmacol. Exp. Ther.* **2004**, *309*, 1124−1131.
(23) Barry, G. D.; Suen, J. Y.; Low, H. B.; Pfeiffer, B.; Flanagan, B.; Halili, M.; Le, G. T.; Fairlie, D. P. A refined agonist pharmacophore for protease activated receptor 2. *Bioorg. Med. Chem. Lett.* **2007**, *17*, 5552−5557.
(24) Boitano, S.; Flynn, A. N.; Schulz, S. M.; Hoffman, J.; Price, T. J.; Vagner, J. Potent agonists of the protease activated receptor 2 (PAR2). *J. Med. Chem.* **2011**, *54*, 1308−1313.
(25) Flynn, A. N.; Hoffman, J.; Tillu, D. V.; Sherwood, C. L.; Zhang, Z.; Patek, R.; Asiedu, M. N.; Vagner, J.; Price, T. J.; Boitano, S. Development of highly potent protease-activated receptor 2 agonists via synthetic lipid tethering. *FASEB J.* **2013**, *27*, 1498−1510.
(26) Barry, G. D.; Suen, J. Y.; Le, G. T.; Cotterell, A.; Reid, R. C.; Fairlie, D. P. Novel agonists and antagonists for human protease activated receptor 2. *J. Med. Chem.* **2010**, *53*, 7428−7440.
(27) Gardell, L. R.; Ma, J. N.; Seitzberg, J. G.; Knapp, A. E.; Schiffer, H. H.; Tabatabaei, A.; Davis, C. N.; Owens, M.; Clemons, B.; Wong, K. K.; Lund, B.; Nash, N. R.; Gao, Y.; Lameh, J.; Schmelzer, K.; Olsson, R.; Burstein, E. S. Identification and characterization of novel small-molecule protease-activated receptor 2 agonists. *J. Pharmacol. Exp. Ther.* **2008**, *327*, 799−808.
(28) Seitzberg, J. G.; Knapp, A. E.; Lund, B. W.; Mandrup Bertozzi, S.; Currier, E. A.; Ma, J. N.; Sherbukhin, V.; Burstein, E. S.; Olsson, R. Discovery of potent and selective small-molecule PAR-2 agonists. *J. Med. Chem.* **2008**, *51*, 5490−5493.
(29) Abad-Zapatero, C.; Metz, J. T. Ligand efficiency indices as guideposts for drug discovery. *Drug Discovery Today* **2005**, *10*, 464−469.
(30) Su, S.; Li, Y.; Luo, Y.; Sheng, Y.; Su, Y.; Padia, R. N.; Pan, Z. K.; Dong, Z.; Huang, S. Proteinase-activated receptor 2 expression in breast cancer and its role in breast cancer cell migration. *Oncogene* **2009**, *28*, 3047−3057.

DOI: 10.1021/acsmedchemlett.5b00429
ACS Med. Chem. Lett. 2016, 7, 105−110